


# Diacylglycerol kinase $\zeta$ limits IL-2-dependent control of PD-1 expression in tumor-infiltrating T lymphocytes

Javier Arranz-Nicolás,<sup>1</sup> Miguel Martin-Salgado,<sup>1</sup> Cristina Rodríguez-Rodríguez,<sup>1</sup> Rosa Liébana,<sup>1</sup> Maria C Moreno-Ortiz,<sup>1</sup> Judith Leitner,<sup>2</sup> Peter Steinberger,<sup>2</sup> Antonia Ávila-Flores,<sup>1</sup> Isabel Merida <sup>1</sup>

**To cite:** Arranz-Nicolás J, Martin-Salgado M, Rodríguez-Rodríguez C, *et al.* Diacylglycerol kinase  $\zeta$  limits IL-2-dependent control of PD-1 expression in tumor-infiltrating T lymphocytes. *Journal for ImmunoTherapy of Cancer* 2020;**8**:e001521. doi:10.1136/jitc-2020-001521

► Additional material is published online only. To view please visit the journal online (<http://dx.doi.org/10.1136/jitc-2020-001521>).

Accepted 05 November 2020



© Author(s) (or their employer(s)) 2020. Re-use permitted under CC BY-NC. No commercial re-use. See rights and permissions. Published by BMJ.

<sup>1</sup>Immunology and Oncology, Centro Nacional de Biotecnología, Madrid, Spain  
<sup>2</sup>Institute of Immunology, Center for Pathophysiology, Infectiology and Immunology, Medical University of Vienna, Wien, Vienna, Austria

**Correspondence to**  
Dr Isabel Merida;  
[imerida@cnb.csic.es](mailto:imerida@cnb.csic.es)

Dr Antonia Ávila-Flores;  
[jaavila@cnb.csic.es](mailto:jaavila@cnb.csic.es)

## ABSTRACT

**Background** The inhibitory functions triggered by the programmed cell death-1 (PD-1) receptor following binding to its ligand (PD-L1) protect healthy organs from cytotoxic T cells, and neutralize antitumor T cell attack. Antibody-based therapies to block PD-1/PD-L1 interaction have yielded notable results, but most patients eventually develop resistance. This failure is attributed to CD8<sup>+</sup> T cells achieving hyporesponsive states from which recovery is hardly feasible. Dysfunctional T cell phenotypes are favored by a sustained imbalance in the diacylglycerol (DAG)- and Ca<sup>2+</sup>-regulated transcriptional programs. In mice, DAG kinase  $\zeta$  (DGK $\zeta$ ) facilitates DAG consumption, limiting T cell activation and cytotoxic T cell responses. DGK $\zeta$  deficiency facilitates tumor rejection in mice without apparent adverse autoimmune effects. Despite its therapeutic potential, little is known about DGK $\zeta$  function in human T cells, and no known inhibitors target this isoform.

**Methods** We used a human triple parameter reporter cell line to examine the consequences of DGK $\zeta$  depletion on the transcriptional restriction imposed by PD-1 ligation. We studied the effect of DGK $\zeta$  deficiency on PD-1 expression dynamics, as well as the impact of DGK $\zeta$  absence on the *in vivo* growth of MC38 adenocarcinoma cells.

**Results** We demonstrate that DGK $\zeta$  depletion enhances DAG-regulated transcriptional programs, promoting interleukin-2 production and partially counteracting PD-1 inhibitory functions. DGK $\zeta$  loss results in limited PD-1 expression and enhanced expansion of cytotoxic CD8<sup>+</sup> T cell populations. This is observed even in immunosuppressive milieu, and correlates with the reduced ability of MC38 adenocarcinoma cells to form tumors in DGK $\zeta$ -deficient mice.

**Conclusions** Our results, which define a role for DGK $\zeta$  in the control of PD-1 expression, confirm DGK $\zeta$  potential as a therapeutic target as well as a biomarker of CD8<sup>+</sup> T cell dysfunctional states.

## BACKGROUND

T cell inhibitory receptors help to sustain self-tolerance, limiting collateral tissue damage during physiological immune responses. These negative regulatory molecules, known as immune checkpoint receptors, represent the main mechanisms of tumor immune

evasion.<sup>1</sup> The potentiation of immune responses to tumors through immune checkpoint targeting (ICT) represents a very promising therapeutic approach.<sup>2</sup> In particular, blocking programmed cell death-1 (PD-1) interaction with its ligands (PD-L1/2) has yielded notable success for the treatment of melanoma and several solid tumors.<sup>3–5</sup> Despite these remarkable results, clinical studies show that more than 40%–65% of melanoma patients present primary resistance to ICT directed to the PD-1/PD-L1 axis, and approximately 43% of initial responders develop acquired resistance by 3 years.<sup>6,7</sup> The greatest challenge to full exploitation of anti-PD-1/PD-L1 blocking therapies is to understand and to develop effective combinations to overcome the mechanisms that trigger resistance. Positive initial responses to anti-PD-1/PD-L1 treatment are associated with increased CD8<sup>+</sup> T cell tumor infiltration. Acquired resistance is attributed mainly to the progressive, sustained promotion of negative signals that eventually drive T lymphocytes into dysfunctional states that closely resemble viral-induced T cell exhaustion.<sup>8</sup> Although PD-1 expression can thus be used to identify antigen-reactive tumor-infiltrating T lymphocytes (TIL),<sup>9</sup> reaching certain levels of PD-1 expression might indicate terminally differentiated dysfunctional T cells.<sup>10</sup>

PD-1 limits T cell receptor (TCR) downstream signaling through recognition of its ligands, expressed on the surface of antigen-presenting cells.<sup>11</sup> Following ligand recognition, tyrosine phosphorylation of the PD-1 cytoplasmic domain by Src family of kinases leads to recruitment of Src homology region 2 domain-containing phosphatases 1 and 2,<sup>12,13</sup> which dephosphorylate signaling molecules downstream of the TCR.<sup>13–15</sup> In healthy cells, robust PD-1 upregulation in response to self-antigens and its signaling via PD-1/

PD-L1 interactions contributes substantially to the early cell fate decisions of CD8<sup>+</sup> T lymphocytes between tolerance and differentiation into cytotoxic T cells (CTL).<sup>16</sup> In cancer, PD-1/PD-L1 triggering facilitates upregulation of additional receptors that limit T cell responses, as well as cytosolic molecules with inhibitory functions.<sup>1</sup> Identifying and targeting key regulatory switches could help to reverse these loops, improving the response to existing therapies.

Anergy and exhaustion are two distinct metabolic T cell states imposed by different mechanisms,<sup>17</sup> but both depend on reduced Ras activation and on facilitated transcription of nuclear factor of activated T cells (NFAT)-regulated genes.<sup>18–20</sup> NFAT-dependent transcription in the absence of activator protein-1 (AP-1) facilitates expression of negative receptors such as TIM3 or LAG3 (18–20), and also upregulates that of E3 ubiquitin ligases, phosphatases, and diacylglycerol (DAG) kinases (DGK), that act at different steps to further limit activation of the pathways that ultimately trigger AP-1 transcription.<sup>21</sup> DGK $\alpha$  and  $\zeta$  isoforms, abundantly expressed in naïve T cells, act as negative regulators of Ras activation downstream of TCR and costimulatory receptors.<sup>22</sup> DGK $\alpha$  and  $\zeta$  are upregulated in tolerant T lymphocytes,<sup>23,24</sup> and their abundance in TIL and engineered CAR T cells correlates with hyporesponsive, anergic states that limit cytotoxic functions.<sup>25,26</sup> Compared with DGK $\alpha$ , DGK $\zeta$  has additional functions that limit the PKC $\theta$ /PDK-1/AKT axis, that in turn regulates nuclear factor  $\kappa$ -light-chain-enhancer of activated B cells (NF $\kappa$ B) activation and mTOR metabolic control downstream of CD28 activation.<sup>27</sup> DGK $\zeta$ -deficient mice show partial but clear resistance to orthotopically implanted tumors,<sup>28–30</sup> suggesting that DGK $\zeta$  inhibition help to re-invigorate exhausted TIL and engineered CAR T cells.<sup>31,32</sup>

In spite of its potential therapeutic value, there is limited information on the effects of DGK $\zeta$  targeting in human T cells, partially as a result of the lack of isoform-specific inhibitors.<sup>31,32</sup> Here, we used the triple parameter reporter (TPR) cell line<sup>33</sup> to investigate the effects of short hairpin interfering RNA (shRNAi)-mediated silencing of DGK $\zeta$  on the regulation of the T cell transcriptional program in conditions of full stimulation or PD-1-dependent inhibition. We confirm that DGK $\zeta$  silencing promotes robust NF $\kappa$ B and AP-1 activation and identify its contribution to NFAT-regulated transcription. Depletion of DGK $\zeta$  does not fully restore PD-1-mediated inhibitory actions in TPR cells that constitutively bear this negative receptor, but greatly limits the extent of PD-1 expression at the early stages of T cell responses. This control of PD-1 expression by DGK $\zeta$  is conserved in mouse CD8<sup>+</sup> T cells, and explains the reduced ability of MC38 colon adenocarcinoma cells to induce tumors when engrafted in DGK $\zeta$ -deficient animals. Our experiments suggest that genetic, and probably pharmacological, manipulation of DGK $\zeta$  alter CD8<sup>+</sup> T cell fate, tipping the balance between effector and tolerant/exhausted cells in the tumor milieu. These data strongly support the therapeutic potential of DGK $\zeta$  and

the need for isoform-specific inhibitors to add to current immunotherapy tools.

## METHODS

### Antibodies and reagents

For pharmacological stimulation, we used phorbol 12-myristate 13-acetate (PMA; Sigma) and ionomycin (Calbiochem). For antibody (Ab)-based stimulation, we used mouse antihuman or hamster antimouse monoclonal anti-CD3 and -CD28 Ab (555336, 555725, 553058, 553295; all from BD Pharmingen). For flow cytometry analyzes, we used LIVE/DEAD fixable red cell death staining kit (L23102, Invitrogen) and antimouse CD45-APC (L23102, eBioscience) or Percp-Cy5.5, CD8-BV610 and CD25-PCy7 (103132, 100744, and 102016, respectively; all from Biolegend), TCR $\beta$ -FITC (732247, Beckman Coulter) and PD-1-APC780 (47998582, eBioscience), antihuman PD-1-APC (17-9969-42, eBioscience) and CD25-PE (A07774, Beckman Coulter) and paraformaldehyde (TedPella). For western blot analysis, we used anti-DGK $\alpha$  (11547-1-AP, ProteinTech), DGK $\zeta$  (105195, Abcam),  $\alpha$  tubulin (T5168, Sigma), GAPDH (G-9, Santa Cruz), horseradish peroxidase-conjugated antimouse and rabbit IgG (P0447, P0260, Dako), antirabbit IgG Dylight 800 (SA5-35571, Invitrogen) and mouse IgG AlexaFluor 680 (175775, AbcamLife). IKK $\beta$  inhibitor PS-1145 was from Sigma-Aldrich, MEK inhibitor PD98059 was from Calbiochem, and calcineurin (CaN) inhibitor FK506 was from Merck Millipore. Anti-PD-1 (nivolumab) humanized Ab was from BioVision. For TIL isolation, we used collagenase type I (Worthington), dispase II and DNase I (both from Roche). Trypsin was from Biowest.

### Cell lines, culture and stimulation

Human Jurkat JE6.1-derived TPR cells, transduced to express NFAT-GFP, NF $\kappa$ B-CFP (cyan fluorescent protein) and AP-1-Cherry, were generated and selected as reported.<sup>33</sup> TPR cells retrovirally transduced with vectors encoding PD-1 were described.<sup>33</sup> Human leukemic Jurkat cells were from ATCC. T cell stimulator (TCS) cells, a murine thymoma cell line (Bw5147) engineered to stably express an antihuman CD3 single-chain fragment anchored to the cell membrane via a human CD14 stem, have been described.<sup>34</sup> TCS cells expressing no human costimulatory molecule were used as control TCS (TCS-control) and compared with cells retrovirally transduced to express human CD86 (TCS-CD86), either alone or in the presence of PD-L1 (TCS-CD86/PD-L1). Murine MC38 adenocarcinoma cell line was a kind gift from Prof. Santos Mañes (CNB-CSIC). All cells were maintained in complete RPMI medium (cRPMI) consisting of RPMI (Invitrogen) supplemented with 10% heat-inactivated fetal bovine serum (FBS; Invitrogen), 1% HEPES (Sigma), 2 mM L-glutamine and penicillin and streptomycin (100 U/mL; Biowest) (37°C, 5% CO<sub>2</sub>).

C57BL/6J-DGK $\zeta$ -deficient mice were reported previously.<sup>35</sup> Lymph nodes were isolated from 6 to 12 weeks

mice. Cells were maintained in cRPMI supplemented with 50 mM  $\beta$ -mercaptoethanol (Merck) (37°C, 5% CO<sub>2</sub>).

For pharmacological/Ab-based stimulation, TPR cells (5 × 10<sup>4</sup>) in 50  $\mu$ L were stimulated in cRPMI medium with PMA (50  $\mu$ M) and ionomycin (1  $\mu$ M; Sigma-Aldrich) for indicated times, or with anti-CD3/CD28 mAb (1  $\mu$ g/mL each) for 24 hours.

For experiments with mouse cells, T lymphocytes were isolated from lymph nodes according to standard protocols and maintained in complete medium throughout the assay. Cells (2.5 × 10<sup>6</sup>) were cultured on anti-CD3 mAb-coated plates with medium containing anti-CD28 mAb (72 hours, 37°C).

For stimulation with TCS cells, TPR or Jurkat cells (5 × 10<sup>4</sup>) were cocultured with TCS cells (2 × 10<sup>4</sup>) in 100  $\mu$ L medium in a 96-well round-bottom plate for the indicated times (37°C, 5% CO<sub>2</sub>). Where indicated, 30  $\mu$ M PS-1145 (IKK $\beta$  inhibitor), 50  $\mu$ M PD98059 (MEK inhibitor), 20 nM FK506 (CaN inhibitor) or 0.5  $\mu$ g/mL anti-PD-1 (nivolumab) was added.

### Flow cytometry analysis

TPR/TCS or Jurkat/TCS cocultures were stained with anti-mouse CD45-APC or Percp-Cy5.5 to exclude TCS cells from analysis. Live cells were gated using forward and side scatter parameters within the CD45<sup>+</sup> subset. Expression of NFAT-GFP, NF $\kappa$ B-CFP and AP-1-Cherry, was determined by flow cytometry analysis of the live cell population using a CytoFLEX S flow cytometer (Beckman Coulter). Mean and SD of the geometric mean fluorescence intensity (gMFI) of the whole population and the percentage of positive cells were determined from triplicate wells. Transcription factor activity was calculated by normalizing data to the maximal activation for each experiment.

Jurkat and LN mouse T cells were washed after stimulation and stained with LIVE/DEAD fixable red cell death staining kit, and stained with a mixture of Ab. Cells isolated from tumors were subjected to the same procedure, in this case CD45 staining was used to exclude MC38 cells from analysis. CD8<sup>+</sup> T cells were identified among total T cells (CD45<sup>+</sup> TCR<sup>+</sup>) and the expression of CD25 and PD-1 evaluated with the corresponding Ab.

Data were analyzed using FlowJo software (V.10.2, FlowJo LLC, Ashland, Oregon, USA).

### Western blot analysis

Cells were lysed and processed as in<sup>27</sup> and western blots probed with specific antibodies. Protein bands were visualized by enhanced chemiluminescence (ECL detection, Amersham Bioscience) or with an Odyssey scanner (LI-COR). Densitometric analysis of proteins was performed using ImageJ.

### Plasmids and transfections

TPR or Jurkat cells in logarithmic growth (4–5 × 10<sup>5</sup> cells/mL) were transfected with 15–20  $\mu$ g plasmid DNA by electroporation using Gene Pulser II (BioRad)

(270 mV, 975  $\mu$ F). For DGK $\zeta$  silencing experiments, a validated sequence for the DGK $\zeta$  isoform was selected to generate the shRNAi pSUPER construct.<sup>27</sup> Equivalent murine sequences were cloned and used as negative controls.<sup>36</sup> Expression was evaluated from days 1 to 4 post-transfection by western blot. Plasmids encoding the interleukin 2 (IL-2) promoter region were reported.<sup>23</sup> The IL-2 promoter was obtained from Addgene. Renilla luciferase vector was from Promega.

### Dual-luciferase reporter assay

TPR cells were transfected with 15  $\mu$ g of the IL-2 promoter construct, with 200 ng renilla as internal control. After 24 hours, cells were washed, allowed to recover (6 hours) and stimulated using TCS cells for 24 hours (37°C, 5% CO<sub>2</sub>). Cells were harvested and assayed for luciferase activity using the Dual-Luciferase Reporter assay (Promega). Luciferase activity was reported relative to renilla luciferase activity.

### IL-2 detection in culture supernatants

Supernatants from TPR/TCS cocultures were collected and IL-2 levels measured using the ELISA MAX Deluxe Set Human IL-2 kit (Biolegend).

### Tumor experiments and TIL isolation

MC38 cells were trypsinized from subconfluent monolayers, washed, and injected subcutaneously in 100  $\mu$ L (5 × 10<sup>5</sup>) into one flank of female 6- to 8-week-old C57BL/6J wild type (wt) or DGK $\zeta$ -deficient mice. Tumor growth was monitored in a blind manner with calipers, and area and volume were estimated according to the formulas: area =  $a \times b$ /volume = (a<sup>2</sup> × b)/2, where  $a$  is tumor width and  $b$  is tumor length in mm. Mice were sacrificed when wt tumors reached 1 cm<sup>3</sup>, at ~19 days postinjection, and tumors were excised, measured and weighed.

For TIL isolation, tumors were fragmented into 1 mm<sup>3</sup> pieces using a scalpel. Fragments were suspended in DMEM culture medium (Invitrogen) supplemented with 20 mM HEPES, with 2 mg/mL collagenase type I, 2.5 mg/mL dispase II and 0.1 mg/mL DNase I, and incubated with gentle shaking (15 min, 37°C). The resulting suspension was filtered with a 70  $\mu$ m filter, washed with PBS+5% FBS and centrifuged (5 min, 300 X g, 4°C). Resulting pellets were processed for flow cytometry analysis.

### Statistical analysis

Flow cytometry data were analyzed with GraphPad Prism V.6 software. Data are shown as mean ± SEM. Samples were assumed to fit normality. When more than two conditions were analyzed, we applied analysis of variance and Bonferroni post-test analysis. If not applicable, parametric unpaired t tests were performed. In all cases, differences were considered statistically not significant (ns) for  $p > 0.05$ , and significant for  $p$  values \* $p < 0.05$ ; \*\* $p < 0.01$ ; \*\*\* $p < 0.001$ ; \*\*\*\* $p < 0.0001$ .

## RESULTS

### The TPR cell model is a useful cell platform to examine the contribution of DAG-regulated signals to functional T cell activation

The TPR cell model allows the concurrent flow cytometry analysis of NFAT, NFκB and AP-1 transcriptional activation.<sup>33</sup> These three transcription factors classically represent the end-point activation of Ca<sup>2+</sup>-dependent CaN activation, as well as of Ras/extracellular signal-regulated kinase (ERK)- and protein kinase C (PKC) θ/IκB kinase (IKK) β-regulated pathways. Flow cytometry analysis of fluorescent proteins coupled to transcription factors enables simultaneous quantification of the signal intensity as determined by the reporter gene induction on a per cell basis (gMFI). The percentage of responding cells reflects the digital characteristics of TCR-delivered signals that ensures scaled T cell responses according to dose and affinity for the antigens encountered.<sup>37</sup> Stimulation of TPR cells with phorbol 12-myristate 13-acetate (PMA) and the Ca<sup>2+</sup> ionophore ionomycin evidenced a strong, uniform cell response with distinct kinetics for the different reporters (figure 1A). The early, robust NFAT induction correlated with its direct nuclear entry as the result of its CaN-dependent dephosphorylation.<sup>38</sup> The induction of NFκB or AP-1, which require successive activation of small GTPases and kinases, accumulated over time (figure 1A).

At difference from the uniform response induced by pharmacological stimulation, 24 hours treatment of TPR cells with agonistic mAb to the TCR-CD3 complex resulted in a small percentage of NFAT-positive and AP-1-positive cells but a higher proportion of NFκB activation (figure 1B). Addition of anti-CD28 mAb increased the activity of the three reporters (figure 1B), especially that of NFκB and AP-1 (figure 1B, middle and right), in accordance with the specific contribution of DAG-regulated pathways downstream of CD28 costimulation.<sup>23</sup>

As described,<sup>33</sup> TPR coculture with control TCS cells (TCS control) promoted strong induction of NFAT and NFκB, with lower AP-1 induction (figure 1C). CD28 stimulation with CD86-expressing TCS cells (TCS-CD86), as shown for the CD80 ligand,<sup>33</sup> further increased expression of the three reporters. Individual transcription factor analysis revealed maximal increase in the frequency of AP-1-expressing cells after costimulation (figure 1D). The effect of CD28 stimulation on a per cell basis was also observed for the three transcription factors, with maximal effect for NFκB expression (figure 1E). Bi-parametric analyzes confirmed a marked increase in the percentage of NFAT/AP-1-expressing cells following incubation with TCS-CD86 cells (online supplemental figure 1). These results add new information to existing data on this model, showing that it accurately reproduces the strict requirement for CD28 engagement to reach the AP-1 transcription threshold.

The activation of CaN in response to Ca<sup>2+</sup> not only triggers NFAT nuclear translocation but also cooperates with PKCθ in NFκB and AP-1 regulation.<sup>39</sup> In

agreement, CaN inhibitor FK506 treatment prevented induction of the three transcription factors (figure 1F). NFAT transcription was independent on the PKCθ/IKKβ signals, as demonstrated by the minimal effect of the IKKβ inhibitor PS-1145. Pharmacological IKKβ blockade nonetheless markedly diminished NFκB and AP-1 activation, in accordance with results from primary human T cells<sup>40</sup> (figure 1F). MEK inhibition by PD98059 limited AP-1 transcription but also partially decreased NFAT and NFκB induction (figure 1F), which confirmed the reported role for MEK, an intermediate kinase of the Ras/ERK axis, in the activation of these two transcription factors.<sup>41 42</sup> Overall, these results confirm the critical requirement for the Ca<sup>2+</sup>/CaN axis, and reveal AP-1 transcriptional activation as the sensor most sensitive to signal limitation.

### DGKζ limits transcriptional activation in TPR cells

Biochemical studies combined with luciferase-based assays demonstrate that DGKζ silencing in Jurkat T cells leads to enhanced Ras/ERK and PKCθ/AKT pathway activation, which translates into enhanced NFκB transcription.<sup>27</sup> The TPR model allowed us to examine the result of DGKζ silencing on the simultaneous activation of NFAT, NFκB and AP-1. We used previously validated shRNAi sequences to attenuate DGKζ expression in TPR cells. DGKζ targeting achieved similar extent of silencing than that reported in Jurkat T cells,<sup>27</sup> without affecting that of DGKα (figure 2A and online supplemental figure 2). Flow cytometry analysis of DGKζ-silenced TPR cells at different times after coculture with TCS-control or TCS-CD86 cells showed an enhanced percentage of NFAT-, NFκB- and AP-1-positive cells that was detected as early as 4–6 hours poststimulation (figure 2B). The effect of DGKζ silencing varied for each transcription factor, with increased NFAT and AP-1 induction at early times that contrasted with the sustained, enhanced activation of NFκB throughout the kinetic course. Analysis on a per cell basis showed no major effect of DGKζ depletion for NFAT induction (figure 2C, left), but exhibited increased NFκB and AP-1 expression (figure 2C, middle and right). As also reported for mAb-stimulated Jurkat cells,<sup>27 43</sup> DGKζ silencing did not replace the CD28 requirement for AP-1 induction (figure 2B–C, right). Analysis of the percentage of cells that coexpressed the three reporters confirmed a marked elevation in DGKζ-silenced cells in response to TCR alone or to TCR/CD28 stimulation (figure 2D). Our results illustrate the utility of fluorescent protein-based TPR cells to demonstrate that, as shown in mice, DGKζ potentially limits the threshold of responding T cells.

### PD-1 triggering restricts transcriptional regulation and IL-2 secretion in TPR cells

Previous studies used the TPR system to demonstrate that PD-1 ligation results in strong NFAT/NFκB downregulation with a minimal effect on AP-1.<sup>33</sup> We used

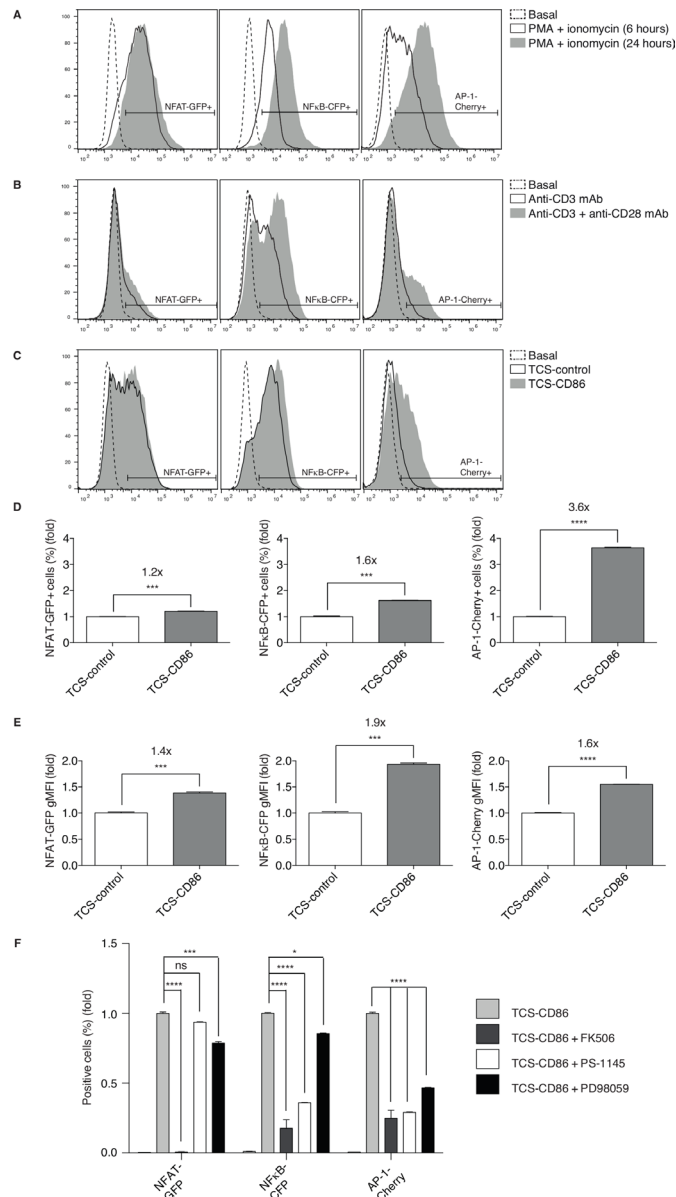


**Figure 1** Functional evaluation of the TPR cell model in response to pharmacological and physiological stimuli. (A–C) NFAT-GFP (left), NFκB-CFP (middle) or AP-1-Cherry (right) induction was analyzed. (A) TPR cells were stimulated using PMA and ionomycin for the indicated times. (B) TPR cells were stimulated using anti-CD3 or anti-CD3/28 mAb for 24 hours. (C) TPR cells were stimulated using TCS-control or TCS-CD86 cells for 24 hours. (D, E) Fold induction of response to TCS-CD86 cells. NFAT-GFP (left), NFκB-CFP (middle) or AP-1-Cherry (right) expressing cell percentage (D) or geometric mean fluorescence intensity (gMFI) (E) was analyzed. TCS-CD86/TCS-control ratios are shown above the graphs. Values are normalized to the TCS control-mediated stimulation condition=1.0. Data were analyzed using parametric unpaired t test; \*\*\* $p < 0.001$ , \*\*\*\* $p < 0.0001$ . (F) Fold induction of response to Ca<sub>v</sub> (FK506), IKKβ (PS-1145) or MEK (PD98059) inhibition in TCS-CD86-stimulated TPR cells. NFAT-GFP, NFκB-CFP or AP-1-Cherry expressing cell percentage was analyzed. Values are normalized to the TCS-CD86-mediated stimulation condition in the absence of inhibitors=1.0. Data were analyzed using two-way ANOVA and Bonferroni post-test; ns  $p > 0.05$ , \*\*\* $p < 0.001$ , \*\*\*\* $p < 0.0001$ . Results are representative of at least three independent experiments with similar results. ANOVA, analysis of variance; AP-1, activator protein-1; NFAT, nuclear factor of activated T cells; NFκB, nuclear factor κ B cells; ns, not significant; TCS, T cell stimulator; TPR, triple parameter reporter.

the same PD-1-expressing TPR (TPR-PD-1) cells, but here we incubated them with TCS cells expressing CD86 alone or in combination with PD-L1 (TCS-CD86/PD-L1) to study the effect of PD-1 ligation in the presence of costimulatory signals. At difference from the effect reported for TCR single stimulation, PD-1 triggering with CD28 costimulation reduced the

percentage (figure 3A) and the expression (figure 3B) of NFAT and AP-1, but had no effect on NFκB activation. These results coincide with the inhibition of TCR-driven early signals by PD-1 engagement as well as with studies showing that, in human T lymphocytes, CD28 promotes NFκB activation in the absence of TCR triggering.<sup>44</sup>

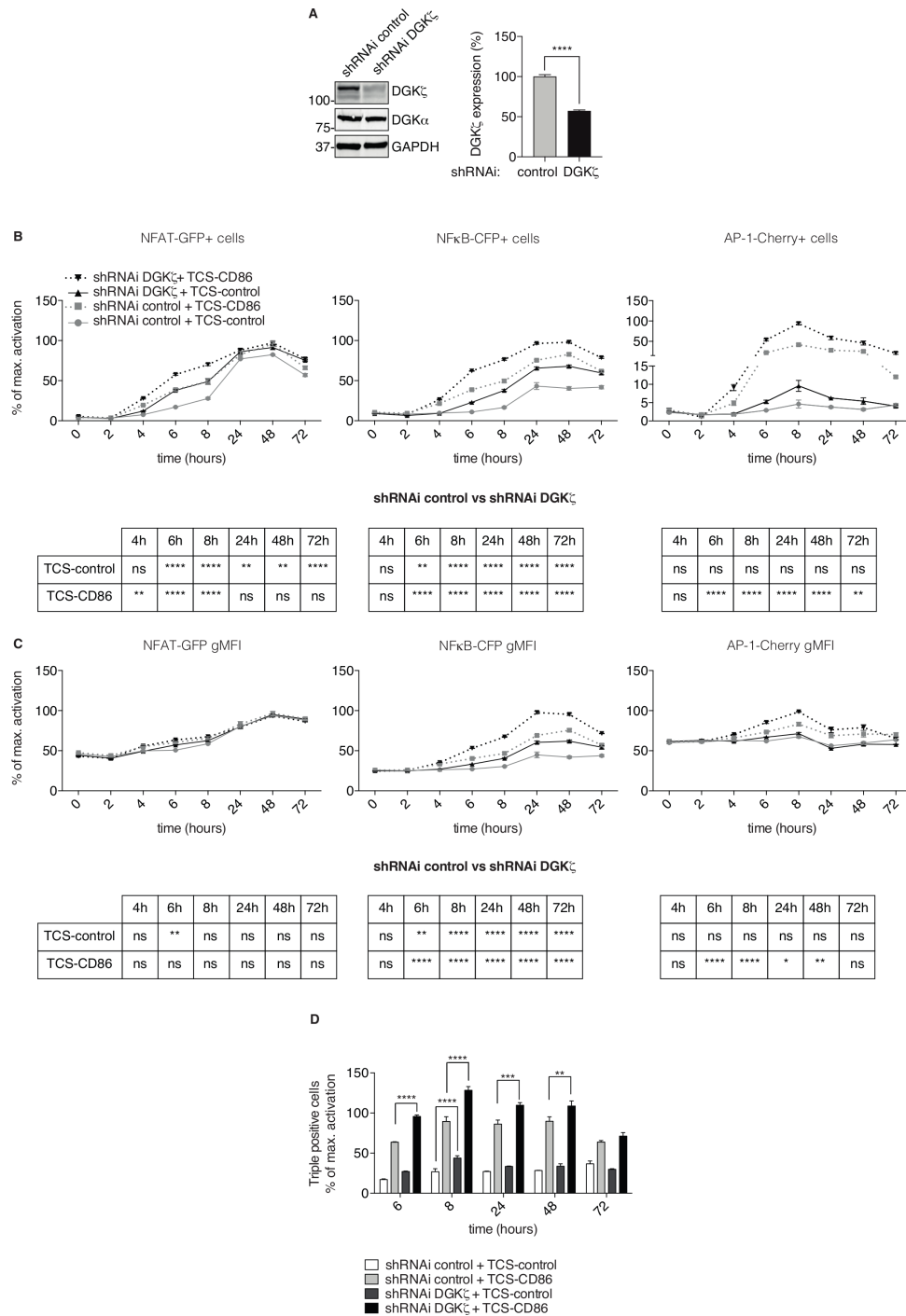


**Figure 2** Effect of DGK $\zeta$  silencing on the transcription factor activity of NFAT, NF $\kappa$ B and AP-1. (A) DGK $\zeta$  was silenced in TPR cells and silencing confirmed by western blot (left), quantification of DGK $\zeta$  expression in control and silenced TPR cells was determined in three independent experiments (right). Control and DGK $\zeta$ -silenced TPR cells were stimulated with TCS-control or TCS-CD86 cells for the indicated times. NFAT-GFP (left), NF $\kappa$ B-CFP (middle) or AP-1-Cherry (right) expressing cell percentage (B) or geometric mean fluorescence intensity (gMFI) (C) was analyzed. (D) Control and DGK $\zeta$ -silenced TPR cells were stimulated with TCS control or TCS-CD86 cells for the indicated times and the percentage of cells simultaneously expressing the three reporters was analyzed. Transcription factor activity was calculated by normalizing data to the maximal activation. Data were analyzed using two-way ANOVA and Bonferroni post-test; ns \* $p > 0.05$ , \*\* $p < 0.01$ , \*\*\* $p < 0.001$ , \*\*\*\* $p < 0.0001$ . The analysis of the experiments represented in B and C, are summarized in the tables below each figure. Results are representative of at least three independent experiments with similar results. AP-1, activator protein-1; DGK, diacylglycerol kinases; NFAT, nuclear factor of activated T cells; NF $\kappa$ B, nuclear factor  $\kappa$  B cells; ns, not significant; shRNAi, short hairpin interfering RNA; TCS, T cell stimulator; TPR, triple parameter reporter.

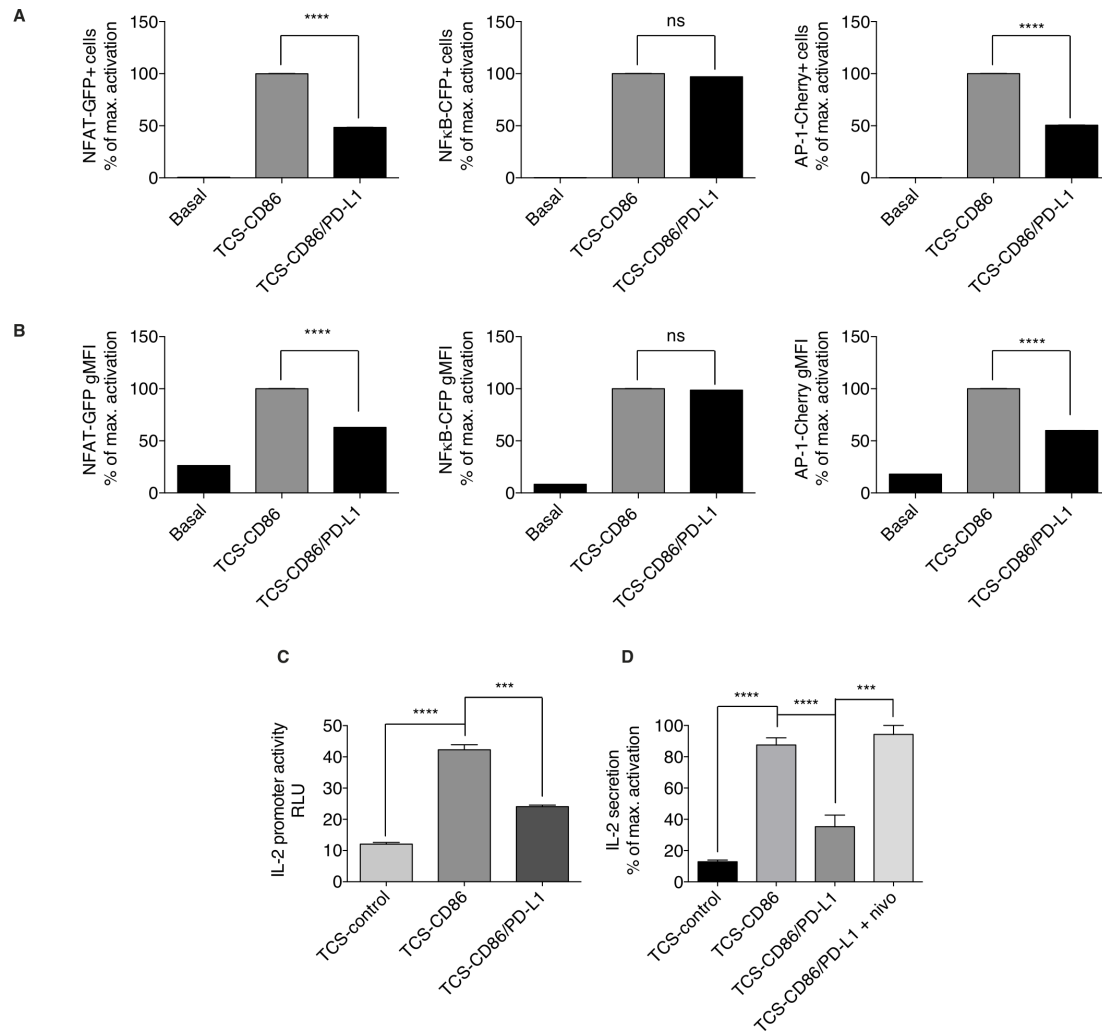


**Figure 3** Effect of PD-1/PD-L1 triggering on transcriptional regulation and secretion of IL-2. (A, B) PD-1 expressing TPR (TPR-PD-1) cells were stimulated using TCS-CD86 or CD86/PD-L1 bearing TCS (TCS-CD86/PD-L1) cells for 24 hours. NFAT-GFP (left), NFκB-CFP (middle) or AP-1-Cherry (right) expressing cell percentage (A) or geometric mean fluorescence intensity (gMFI) (B) was analyzed. Transcription factor activity was calculated by normalizing data to the maximal activation. (C) Luciferase activity of an IL-2 reporter construct was determined in TPR-PD-1 cells stimulated with TCS-control, TCS-CD86 or TCS-CD86/PD-L1 cells for 24 hours. Luciferase activity was corrected using an internal renilla luciferase control. (D) IL-2 secretion to medium was assessed in supernatants of TPR-PD-1 cells stimulated with TCS-control, TCS-CD86 or TCS-CD86/PD-L1 cells for 24 hours. When indicated, a humanized anti-PD-1 antibody (nivolumab (nivo)) was added. IL-2 secretion was calculated by normalizing data to the maximal activation. Data were analyzed using parametric unpaired t-test (A, B) or one-way ANOVA and Bonferroni post-test (C, D); NS  $^{***}p < 0.001$ ,  $^{****}p < 0.0001$ . Results are representative of at least three independent experiments with similar results. ANOVA, analysis of variance; IL-2, interleukin 2; NFAT, nuclear factor of activated T cells; NFκB, nuclear factor κ B cells; ns, not significant; PD-1/PD-L1, programmed cell death-1/ligand 1; TCS, T cell stimulator; TPR, triple parameter reporter.

Correct and timely coordinated activation of NFAT, NFκB and AP-1 is indispensable for transcription of IL-2, which orchestrates the ensuing clonal expansion of effector populations.<sup>45</sup> Analysis of a luciferase-coupled IL-2 promoter in TPR-PD-1 cells demonstrated the need for CD28 stimulation, and confirmed the PD-1-driven limitation of IL-2 transcription (figure 3C). Determination of IL-2 secretion by stimulated cells fully reflected the observations in the promoter experiments; only those cells stimulated by TCS-CD86 cells showed robust secretion of this cytokine, which was greatly restricted by PD-1/PD-L1 ligation (figure 3D).

These results confirm a strict requirement for CD28 triggering to reach the correct AP-1 threshold, which acts in concert with NFAT and NFκB,<sup>46 47</sup> and the limitation on IL-2 production imposed by PD-1 engagement, even in the presence of costimulatory signals.<sup>48</sup> TPR-PD-1 cells stimulated with TCS-CD86/PD-L1 cells restored IL-2 production after incubation with an anti-PD-1 humanized Ab (nivolumab, nivo) (figure 3D). Our analyzes confirm the utility of the TPR cell model to reproduce the specific PD-1 contribution to T cell hyporesponsive states, as well as the effect of blocking antibodies used in the clinic.

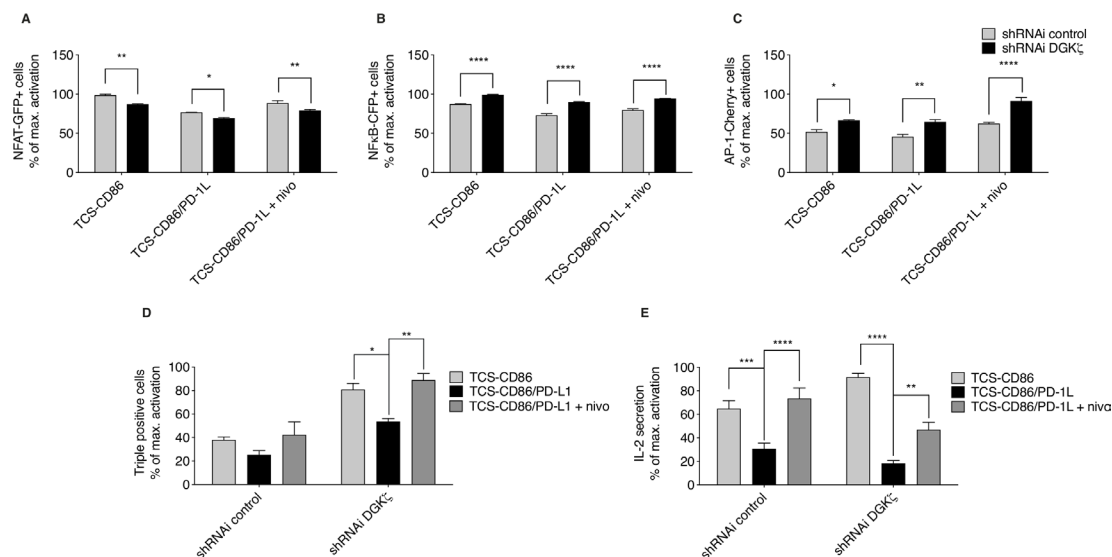


**Figure 4** Effect of DGK $\zeta$  silencing on the transcriptional restrictions imposed by PD-1/PD-L1 triggering. (A–D) Control or DGK $\zeta$ -silenced TPR-PD-1 cells were stimulated with TCS-CD86 or TCS-CD86/PD-L1 cells for 24 hours. (A–D) NFAT-GFP (left), NF $\kappa$ B-CFP (middle) or AP-1-Cherry (right), or triple expressing cell percentage (D) was analyzed. Transcription factor activity was calculated by normalizing data to the maximal activation. (E) IL-2 secretion to medium was assessed in supernatants of control or DGK $\zeta$ -silenced TPR-PD-1 cells stimulated with TCS-CD86 or TCS-CD86/PD-L1 cells for 24 hours. When indicated, a humanized anti-PD-1 antibody (nivolumab (nivo)) was added. IL-2 secretion was calculated by normalizing data to the maximal activation. Data were analyzed using one-way ANOVA and Bonferroni post-test; \* $p < 0.5$ , \*\* $p < 0.01$ , \*\*\* $p < 0.001$ , \*\*\*\* $p < 0.0001$ . Results are representative of at least three independent experiments with similar results. ANOVA, analysis of variance; DGK, diacylglycerol kinases; IL-2, interleukin 2; NFAT, nuclear factor of activated T cells; NF $\kappa$ B, nuclear factor  $\kappa$  B cells; ns, not significant; PD-1/PD-L1, programmed cell death-1/ligand 1; shRNAi, short hairpin interfering RNA; TCS, T cell stimulator; TPR, triple parameter reporter.

#### DGK $\zeta$ contributes to PD-1 inhibitory effects on AP-1-dependent transcription

We investigated the effect of DGK $\zeta$  silencing in the context of PD-1 inhibitory function. As observed in TPR cells, DGK $\zeta$  silencing in TPR-PD-1 cells increased the frequencies of NF $\kappa$ B- and AP-1-expressing cells, but diminished that of NFAT, compared with control cells (figure 4A–C). PD-1 ligation decreased NFAT transcription both in control and DGK $\zeta$ -silenced cells (figure 4A), and had no obvious effect on NF $\kappa$ B induction (figure 4B). Nivolumab-mediated blockade of PD-1/PD-L1 interaction restored NFAT in control and DGK $\zeta$ -silenced cells (figure 4A). Compared with control cells, DGK $\zeta$ -silenced cells showed less sensitivity to PD-1-dependent AP-1 inhibition and displayed further induction of AP-1 following nivolumab treatment (figure 4C). Although the effects of DGK $\zeta$  silencing were small in the analysis of each independent transcription factor, the evaluation of percentage of TPR-PD-1 cells that coexpressed the three reporters confirmed a significantly higher proportion of responding cells following DGK $\zeta$  silencing, which nonetheless decreased after PD-1 triggering and was fully restored by nivolumab treatment (figure 4D). The biological significance of these changes was reflected by the analysis of IL-2 secretion, which confirmed enhanced IL-2 production by DGK $\zeta$ -silenced TPR-PD-1 cells (figure 4E). DGK $\zeta$  silencing did not confer resistance to PD-1 engagement, resulting in severe impairment of IL-2 secretion, with partial

but significant recovery following nivolumab addition (figure 4E).

#### DGK $\zeta$ promotes PD-1 expression by limiting IL-2 in activated T cells

The previous experiments demonstrate the utility of the TPR model for studying the contribution of DGK $\zeta$ -regulated pathways in the activation of positive and negative receptors in human T cells, and suggest that this platform could be used to profile isoform-specific DGK inhibitors. TPR cells are nonetheless an artificial system in which receptors can be analyzed at a fixed level of expression. Naïve T cells do not constitutively express PD-1, which is induced following activation.<sup>49</sup> PD-1-mediated inhibition depends on TCR signal strength, with greater inhibition at low levels of TCR stimulation.<sup>50</sup> In line with this fact, PD-1-delivered inhibition can be overcome by CD28<sup>51</sup> or IL-2.<sup>48</sup> IL-2 production in response to CD28 engagement is central to CD28 ability to rescue from PD-1-driven negative regulation.<sup>48</sup> IL-2 leads to cell expansion by ensuring expression of CD25, which constitutes the high affinity receptor for this cytokine. We studied the kinetics of CD25 and PD-1 induction in Jurkat T cells stimulated with PMA and ionomycin or TCS-CD86 cells. As shown, both proteins were rapidly induced as early as 6 hours in response to both stimuli (figure 5A–C). In agreement with IL-2-dependent regulation of both proteins,<sup>52</sup> by 24 hours CD25 expression was further increased, whereas PD-1 expression was reduced (figure 5A–C).



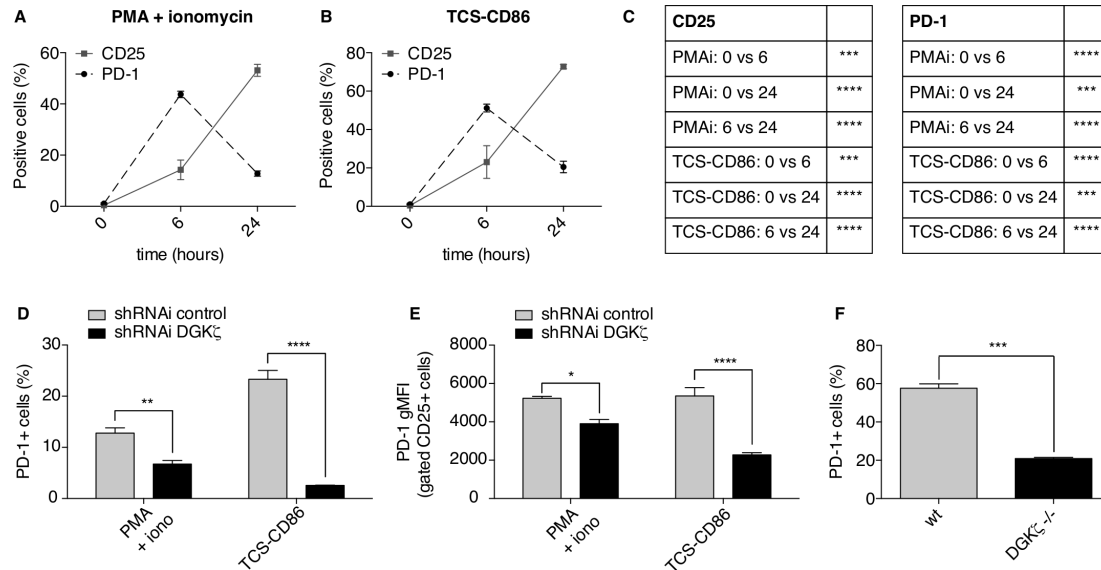


**Figure 5** Stronger IL-2-dependent signals in DGK $\zeta$ -deficient CD8<sup>+</sup> T cells limit PD-1 expression. (A–C) Parental Jurkat cells were stimulated with PMA and ionomycin (PMAi) (A) or TCS-CD86 (B) for the indicated times. CD25 or PD-1 expressing cell percentage was analyzed. In C, the results of the comparisons are summarized in the table. D–E. DGK $\zeta$  was silenced in Jurkat cells. Control or DGK $\zeta$ -silenced Jurkat cells were stimulated with PMA and ionomycin (iono) or TCS-CD86 for 24 hours. PD-1 expressing cell percentage (D) or gMFI within CD25<sup>+</sup> cells (E) was analyzed. (F) wt or DGK $\zeta$ -deficient primary CD8<sup>+</sup> T cells were stimulated with plate-bound anti-CD3 mAb and soluble anti-CD28 mAb for 72 hours. PD-1 expressing cell percentage was analyzed. Data were analyzed using two-way ANOVA and Bonferroni post-test (A–E) or parametric unpaired t test (F); \* $p < 0.1$ , \*\* $p < 0.01$ , \*\*\* $p < 0.001$ , \*\*\*\* $p < 0.0001$ . Results are representative of at least three independent experiments with similar results. ANOVA, analysis of variance; DGK, diacylglycerol kinases; gMFI, geometric mean fluorescence intensity; IL-2, interleukin 2; PD-1, programmed cell death-1; shRNAi, short hairpin interfering RNA; TCS, T cell stimulator; wt, wild type.

Concurring with its function as a negative regulator of CD28 signals, DGK $\zeta$  silencing further reduced the percentage of PD-1<sup>+</sup> Jurkat cells (figure 5D). The decrease in PD-1 expression was particularly marked in the CD25<sup>+</sup> T cell population (figure 5E). Consistent with observations in the Jurkat model, stimulation of mouse T cells from DGK $\zeta$ -deficient mice also led to a notable reduction in the percentage of PD-1<sup>+</sup> CD8<sup>+</sup> T cells compared with wt mice (figure 5F). These results indicate conservation in human and mouse T lymphocytes of a positive feedback by which DGK $\zeta$  promotes PD-1 expression and negative function.

#### DGK $\zeta$ deficiency reduces *in vivo* growth of MC38 colon adenocarcinoma cells, a PD-1-related tumor model

Antigen recognition facilitates PD-1 upregulation in TIL, whereas PD-L1 expression by tumor or stromal cells increases the probability of PD-1 ligation.<sup>10</sup> This leads to a scenario in which IL-2 production is reduced and the expansion of CD8<sup>+</sup> CTL populations is limited.<sup>13</sup> Our previous observations showing a correlation between enhanced IL-2 production and reduced PD-1 expression as a result of DGK $\zeta$  depletion might be a plausible mechanism to explain the enhanced control of engrafted tumors observed in DGK $\zeta$ -deficient mice.<sup>28–30</sup> Although the Jurkat cell line is a good platform in which to study cytokine production, these cells lack cytotoxic abilities. We, thus, moved to mouse models that facilitate the examination of the DGK $\zeta$  modulation of antitumor T cell functions.

At difference from findings in human colorectal tumors, which are in most cases PD-1-resistant, the induction of orthotopic tumors in mice by subcutaneous injection of MC38 adenocarcinoma cells is a classical model of sensitivity to PD-1/PD-L1 immune checkpoint blockade.<sup>53</sup> We selected this tumor model to test whether the observed modulation of the CD25/PD-1 axis by DGK $\zeta$  could affect tumor development. Analysis of growth kinetics of MC38 engrafted cells showed a notable growth lag in DGK $\zeta$ -deficient mice, which developed considerably smaller tumors than those in wt animals by the time at which they had to be sacrificed (figure 6A–B). We explored existing differences in CD25<sup>+</sup> and PD-1<sup>+</sup> CD8<sup>+</sup> T cell populations in TIL isolated from tumors implanted in wt and DGK $\zeta$ -deficient mice. TIL analysis showed similar percentage of live (figure 6C) and CD45<sup>+</sup> cells (figure 6D) with a tendency, not statistically significant, of higher CD8<sup>+</sup> T cell percentage in TIL isolated from tumors in DGK $\zeta$ -deficient mice (figure 6E). TIL isolated from tumors grown in DGK $\zeta$ -deficient mice showed a significant increase in CD25<sup>+</sup> CD8<sup>+</sup> T cell frequency (figure 6F) and in CD25 expression per cell (figure 6G) compared with those from wt mice. TIL analysis showed no marked differences in the percentage of PD-1<sup>+</sup> CD8<sup>+</sup> T cells (figure 6H) but, in agreement with findings in Jurkat and mouse T cells, PD-1 expression specifically in the CD25<sup>+</sup> CD8<sup>+</sup> T cell population was lower in TIL from DGK $\zeta$ -deficient

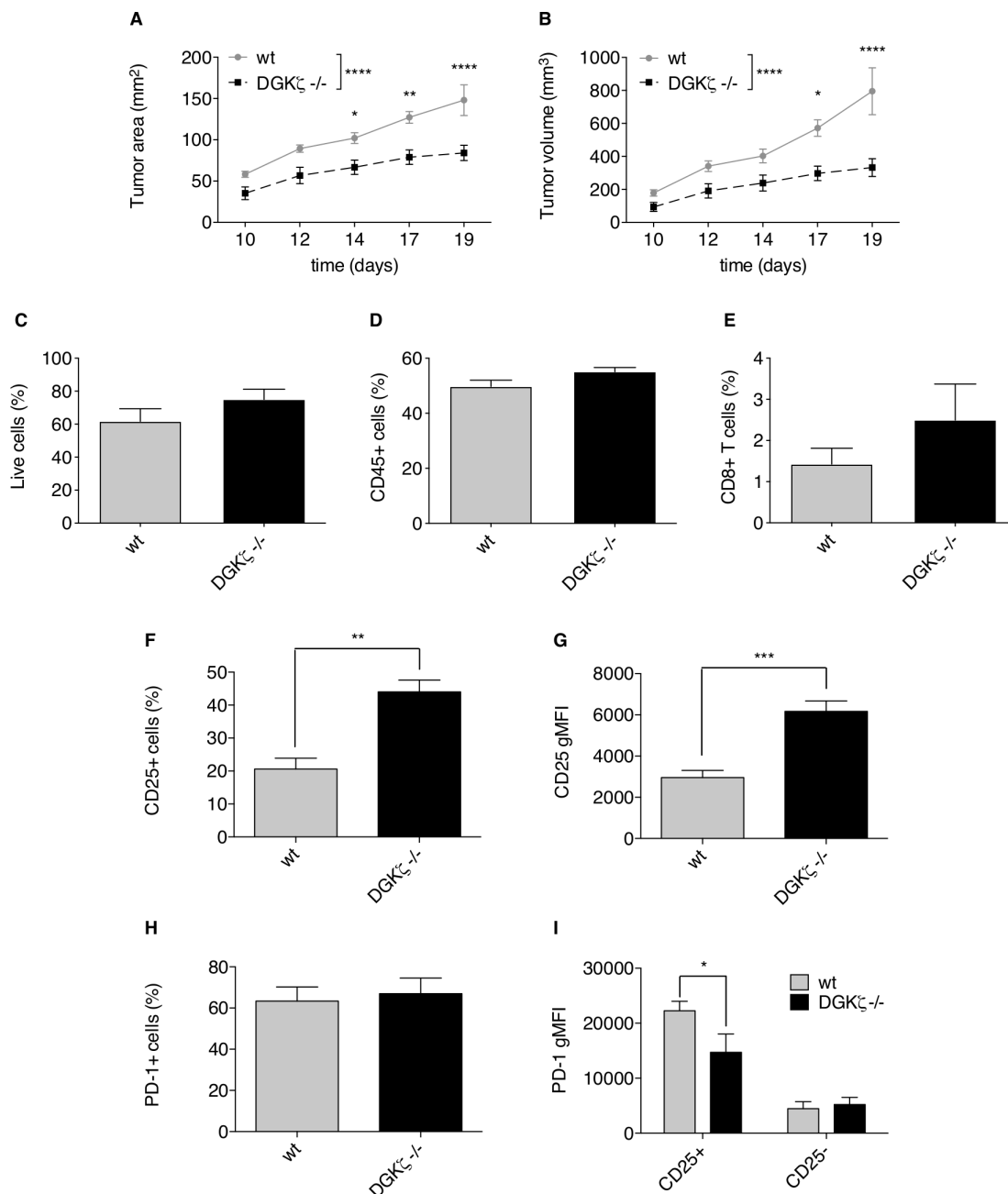


**Figure 6** DGK $\zeta$  deficiency limits MC38 tumor growth favoring expansion of CD8<sup>+</sup>CD25<sup>+</sup> T cell populations. wt or DGK $\zeta$ -deficient mice received subcutaneous injections of  $5 \times 10^5$  MC38 colon adenocarcinoma cells. (A, B) Tumor progression was evaluated daily until wt animals had to be sacrificed following standards imposed by CNB-CSIC Ethics Committee for Animal Experimentation were reached by day 19. Tumor area (A) or volume (B) was analyzed. Tumors from wt or DGK $\zeta$ -deficient mice were excised and cells analyzed by flow cytometry. (C–I) The percentage of live (C), CD45<sup>+</sup> (D) and CD8<sup>+</sup> T (E) cells were compared. CD25 expressing cell percentage (F) or gMFI (G) within the whole CD8<sup>+</sup> T cell population was analyzed. PD-1 expressing cell percentage within the whole CD8<sup>+</sup> T cell population (H) was analyzed. PD-1 gMFI was analyzed within the CD8<sup>+</sup>CD25<sup>+</sup> or CD8<sup>+</sup>CD25<sup>-</sup> T cell subsets. Data were analyzed using two-way ANOVA and Bonferroni post-test (A, B, I) or parametric unpaired t-test (C–H); \* $p < 0.05$ , \*\* $p < 0.01$ , \*\*\* $p < 0.001$ , \*\*\*\* $p < 0.0001$ . Results are representative of at least three independent experiments with similar results. ANOVA, analysis of variance; DGK, diacylglycerol kinases; gMFI, geometric mean fluorescence intensity; PD-1, programmed cell death-1; wt, wild type.

than in those from wt mice (figure 6I). These results confirm a role for DGK $\zeta$  in limiting effector functions, and suggest DGK $\zeta$  targeting as a potential means to avoid exhausted T cell phenotypes, even in the context of immunosuppressive milieus.

## DISCUSSION

DGK $\zeta$ -dependent transformation of DAG into phosphatidic acid limits the activation of the RasGRP1/Ras-regulated and PKC $\theta$ -regulated pathways. This reaction maintains correct spatiotemporal coordination of these

signaling pathways that ultimately guarantees an appropriate immune response.<sup>54</sup> Abnormal upregulation of DGK $\zeta$  in primary T cells and/or engineered CAR T cells that infiltrate solid tumors leads to hyporesponsive states that facilitate tumor immune evasion during tumor escape.<sup>55</sup> Targeting DGK $\zeta$  activity thus offers interesting therapeutic possibilities for cancer immunotherapy, but design of successful approaches demands identification of its functional interactors. In this study, we establish that DGK $\zeta$  and PD-1 operate in a positive feedback loop in which DGK $\zeta$  contributes to sustain PD-1 expression, leading to the onset of inhibitory functions that ultimately facilitate immune evasion.

Using the TPR cell model, we corroborated previous mouse data that linked DGK $\zeta$  with control of NF $\kappa$ B and AP-1 activity,<sup>27</sup> and found that DGK $\zeta$  also negatively controls NFAT transcription. Although the mechanisms that support this last connection remain to be explored, our observations in cells in which DGK $\zeta$  expression is only partially attenuated provide additional clues to explain the strong potentiating effects observed in genetically deficient mice. The use of CD86-expressing TCS cells confirms the relevance of CD28-driven signals for stabilization of AP-1 induction, in agreement with earlier observations.<sup>56</sup> Together with NFAT and NF $\kappa$ B, AP-1 regulates the transcription of cytokines and cell surface receptors that facilitate T cell cycle entry, clonal expansion, and anergy avoidance.<sup>57 58</sup> Accordingly, only TPR cells cocultured with TCS-CD86 showed noticeable IL-2 transcription and secretion. The TPR model thus provides a reliable, easy to manipulate, robust cellular platform that reproduces the requirements for IL-2 production, the hallmark of clonal expansion that follows T cell activation.

Constitutive PD-1 expression in TPR-PD-1 cells did not alter CD28 costimulatory signals, but simultaneous triggering of the two receptors by use of CD86/PD-L1-bearing TCS cells markedly abrogated IL-2 production, which was reinstated by the anti-PD-1 blocking Ab nivolumab.<sup>59</sup> This genuinely reproduces the PD-1 inhibitory effects on CD28-triggered costimulatory functions,<sup>60</sup> and confirms the potential of this platform for use in trials to test combinatorial treatments, and in the search for inhibitors that target T cell response modulators such as DGK $\zeta$ .

Dual stimulation of PD-1 and CD28 provides interesting conclusions regarding the effect of PD-1 triggering on CD28-dependent signals. Whereas PD-1 ligation reduced NFAT and AP-1 induction, we observed no repression of NF $\kappa$ B activation. These results correlate well with the CD28 ability to elicit NF $\kappa$ B activation in the absence of TCR triggering in human T cells.<sup>44</sup> Interestingly, DGK $\zeta$ -silenced cells showed resistance to PD-1-dependent inhibition of AP-1, which confirms the role of this enzyme as a negative regulator of the Ras/ERK pathway in anergic/exhausted T cells. This nonetheless does not preclude inhibition of IL-2 production, suggesting that diminishing DGK $\zeta$  is not enough to counteract the potent limitation imposed by PD-1 triggering.

Although useful in the search for pharmacological inhibitors, the TPR model is an artificial system in which the effect of DGK $\zeta$  silencing can only be explored in conditions of constitutive PD-1 expression. DGK $\zeta$  deficiency in mouse and Jurkat T cells facilitates enhanced IL-2 expression<sup>27</sup> that, as we demonstrate here, limits PD-1 expression, linking this DGK isoform to the control of this immune checkpoint. This explains the partial insensitivity to PD-1/PD-L1-derived immunosuppression observed in DGK $\zeta$ -deficient T cells.<sup>61</sup> It might also have clinical implications. The success of anti-PD-1 therapies is described to be dependent on PD-1 expression not surpassing a determined threshold.<sup>10</sup> Targeting DGK $\zeta$  could limit PD-1 expression, and thus favor the effectiveness of anti-PD-1 blocking therapies. Our observations also suggest the possibility of using DGK $\zeta$  expression as a biomarker in the clinic, especially in those cases in which ICT directed to the PD-1/PD-L1 axis are used, either to monitor the success of these therapies or when resistances to them are developed.

The DGK $\zeta$ -imposed negative control of IL-2 production translates to enhanced PD-1 expression, an observation that fully correlates with the identification of DGK $\zeta$  as a gene upregulated during tolerance induction.<sup>62</sup> The DGK $\zeta$  contribution to CD8<sup>+</sup> T cell fate decisions between tolerance and CTL differentiation provides a mechanistic explanation for the notably diminished growth of MC38 adenocarcinoma cells in DGK $\zeta$ -deficient mice. The MC38 tumor model is highly dependent on PD-1/PD-L1-mediated immunosuppression.<sup>53 63 64</sup> DGK $\zeta$ -deficient TIL analyzes confirmed significant presence of functionally activated CTL, identified as CD25<sup>+</sup> CD8<sup>+</sup> T cells. Our combined assessment of CD25 and PD-1 expression shows reduced PD-1 expression within CD25<sup>+</sup> CD8<sup>+</sup> T cells, which confirms that DGK $\zeta$  deletion facilitates strong T cell responses even in the context of immunosuppressive milieus. In spite of the marked differences in tumor growth, single analysis of PD-1 expression in TIL indicated similar percentages of PD-1<sup>+</sup> CD8<sup>+</sup> T cells in wt and DGK $\zeta$ -deficient mice. Whereas this observation fully agrees with induction of PD-1 expression following T cell activation,<sup>50</sup> our experiments cast doubt on the use of PD-1 single expression studies to monitor T cell responses.

In addition to DGK $\zeta$ , TIL also upregulate DGK $\alpha$ . Studies in human and mouse CAR T cells demonstrate enhanced functions following individual silencing of each isoform.<sup>29 65</sup> These data contrast with the predominant function of DGK $\zeta$  in the control of ERK activation, also observed in CAR T cells.<sup>65</sup> A role for DGK $\alpha$  as a negative regulator of CD8<sup>+</sup> cytotoxic functions was nonetheless previously characterized in mouse models. DGK $\alpha$ -deficient CD8<sup>+</sup> T cells show increased proliferation that correlates with increased production of cytotoxic molecules such as perforin.<sup>66</sup> Individual silencing of DGK $\alpha$  or DGK $\zeta$  in human CAR T cells fails to improve antitumor effects in vivo. Only dual DGK-silenced CAR T cells show enhanced tumor control and higher T cell infiltration.

This observation correlates with the synergistic effect on cytokine production,<sup>65</sup> and suggests safeguarding properties for the individual DGK. Dual targeting of DGK $\alpha$  and  $\zeta$  could constitute a powerful strategy for improving CAR T cell efficiency in solid tumors, particularly in those cases refractory to immune checkpoint blockade.

Our experiments confirm data from mouse studies regarding DGK $\zeta$  depletion-derived effects in a robust, reliable human T cell platform. The results also extend knowledge of the DGK $\zeta$  role in limiting T cell responses, specifically of the DGK $\zeta$  interrelation with an important immune checkpoint such as PD-1; these findings indicate a promising horizon to be explored for further success of cancer immunotherapies.

**Acknowledgements** We thank all members of the Mérida Lab for discussion and suggestions and C. Mark for expert editorial assistance.

**Contributors** Conceptualization: JA-N, AA-F and IM. Generation of TPR and TCS cells: JL and PS. TPR cell experiments: JA-N and AA-F. Mouse experiments: JA-N. Jurkat cell experiments: JA-N and CR-R. MC38 tumor cell engraftment: MM-S and RL. TIL isolation experiments: RL and AA-F. Development and optimization of flow cytometry protocols for TIL studies: MCM-O and AA-F. Writing manuscript: JA-N, AA-F and IM. All authors read and gave input on the manuscript.

**Funding** This work was supported in part by grants from the MINECO (PID2019-108357RB-I00) to AA-F and IM and MINECO (BFU2016-77207-R), the Spanish Association Against Cancer (AECC-1518), the Madrid regional government (IMMUNOTHERCAM Consortium B2017/BMD-3733) and the Aplastic Anemia and MDS International Foundation (AAMDSIF OPE01644), to IM. CR-R is a predoctoral fellow of the Álvaro Entrecanales and Jerome Lejeune Foundations.

**Competing interests** None declared.

**Patient consent for publication** Not required.

**Ethics approval** Protocols approved by the CNB-CSIC Ethics Committee on Animal Experimentation.

**Provenance and peer review** Not commissioned; externally peer reviewed.

**Data availability statement** All data relevant to the study are included in the article or uploaded as online supplemental information.

**Supplemental material** This content has been supplied by the author(s). It has not been vetted by BMJ Publishing Group Limited (BMJ) and may not have been peer-reviewed. Any opinions or recommendations discussed are solely those of the author(s) and are not endorsed by BMJ. BMJ disclaims all liability and responsibility arising from any reliance placed on the content. Where the content includes any translated material, BMJ does not warrant the accuracy and reliability of the translations (including but not limited to local regulations, clinical guidelines, terminology, drug names and drug dosages), and is not responsible for any error and/or omissions arising from translation and adaptation or otherwise.

**Open access** This is an open access article distributed in accordance with the Creative Commons Attribution Non Commercial (CC BY-NC 4.0) license, which permits others to distribute, remix, adapt, build upon this work non-commercially, and license their derivative works on different terms, provided the original work is properly cited, appropriate credit is given, any changes made indicated, and the use is non-commercial. See <http://creativecommons.org/licenses/by-nc/4.0/>.

#### ORCID iD

Isabel Merida <http://orcid.org/0000-0003-2762-6241>

#### REFERENCES

- Pardoll DM. The blockade of immune checkpoints in cancer immunotherapy. *Nat Rev Cancer* 2012;12:252–64.
- Couzin-Frankel J. Breakthrough of the year 2013. *Cancer immunotherapy*. *Science* 2013;342:1432–3.
- Brahmer JR, Drake CG, Wollner I, et al. Phase I study of single-agent anti-programmed death-1 (MDX-1106) in refractory solid tumors: safety, clinical activity, pharmacodynamics, and immunologic correlates. *J Clin Oncol* 2010;28:3167–75.
- Haanen JBAG, Robert C. Immune checkpoint inhibitors. *Prog Tumor Res* 2015;42:55–66.
- Patnaik A, Kang SP, Rasco D, et al. Phase I study of pembrolizumab (MK-3475; anti-PD-1 monoclonal antibody) in patients with advanced solid tumors. *Clin Cancer Res* 2015;21:4286–93.
- Koyama S, Akbay EA, Li YY, et al. Adaptive resistance to therapeutic PD-1 blockade is associated with upregulation of alternative immune checkpoints. *Nat Commun* 2016;7:10501.
- Shin DS, Ribas A. The evolution of checkpoint blockade as a cancer therapy: what's here, what's next? *Curr Opin Immunol* 2015;33:23–35.
- Sharpe AH, Wherry EJ, Ahmed R, et al. The function of programmed cell death 1 and its ligands in regulating autoimmunity and infection. *Nat Immunol* 2007;8:239–45.
- Gros A, Robbins PF, Yao X, et al. PD-1 identifies the patient-specific CD8<sup>+</sup> tumor-reactive repertoire infiltrating human tumors. *J Clin Invest* 2014;124:2246–59.
- Ngiow SF, Young A, Jacquelin N, et al. A threshold level of Intratumor CD8<sup>+</sup> T-cell PD1 expression dictates therapeutic response to anti-PD1. *Cancer Res* 2015;75:3800–11.
- Okazaki T, Chikuma S, Iwai Y, et al. A rheostat for immune responses: the unique properties of PD-1 and their advantages for clinical application. *Nat Immunol* 2013;14:1212–8.
- Chemnitz JM, Parry RV, Nichols KE, et al. SHP-1 and SHP-2 associate with immunoreceptor tyrosine-based switch motif of programmed death 1 upon primary human T cell stimulation, but only receptor ligation prevents T cell activation. *J Immunol* 2004;173:945–54.
- Yokosuka T, Takamatsu M, Kobayashi-Imanishi W, et al. Programmed cell death 1 forms negative costimulatory microclusters that directly inhibit T cell receptor signaling by recruiting phosphatase SHP2. *J Exp Med* 2012;209:1201–17.
- Parry RV, Chemnitz JM, Frauwirth KA, et al. CTLA-4 and PD-1 receptors inhibit T-cell activation by distinct mechanisms. *Mol Cell Biol* 2005;25:9543–53.
- Patsoukis N, Brown J, Petkova V, et al. Selective effects of PD-1 on Akt and Ras pathways regulate molecular components of the cell cycle and inhibit T cell proliferation. *Sci Signal* 2012;5:ra46.
- Goldberg MV, Maris CH, Hipkiss EL, et al. Role of PD-1 and its ligand, B7-H1, in early fate decisions of CD8 T cells. *Blood* 2007;110:186–92.
- McLane LM, Abdel-Hakeem MS, Wherry EJ. CD8 T cell exhaustion during chronic viral infection and cancer. *Annu Rev Immunol* 2019;37:457–95.
- Fehr T, Lucas CL, Kurtz J, et al. A CD8 T cell-intrinsic role for the calcineurin-NFAT pathway for tolerance induction in vivo. *Blood* 2010;115:1280–7.
- Heissmeyer V, Macián F, Im S-H, et al. Calcineurin imposes T cell unresponsiveness through targeted proteolysis of signaling proteins. *Nat Immunol* 2004;5:255–65.
- Martinez GJ, Pereira RM, Ajijó T, et al. The transcription factor NFAT promotes exhaustion of activated CD8<sup>+</sup> T cells. *Immunity* 2015;42:265–78.
- Macián F, García-Cózar F, Im S-H, et al. Transcriptional mechanisms underlying lymphocyte tolerance. *Cell* 2002;109:719–31.
- Mérida I, Andradá E, Gharbi SI, et al. Redundant and specialized roles for diacylglycerol kinases  $\alpha$  and  $\zeta$  in the control of T cell functions. *Sci Signal* 2015;8:re6.
- Macián F, García-Rodríguez C, Rao A. Gene expression elicited by NFAT in the presence or absence of cooperative recruitment of fos and Jun. *Embo J* 2000;19:4783–95.
- Zheng Y, Zha Y, Driessens G, et al. Transcriptional regulator early growth response gene 2 (Egr2) is required for T cell anergy in vitro and in vivo. *J Exp Med* 2012;209:2157–63.
- Moon EK, Wang L-C, Dolfi DV, et al. Multifactorial T-cell hypofunction that is reversible can limit the efficacy of chimeric antigen receptor-transduced human T cells in solid tumors. *Clin Cancer Res* 2014;20:4262–73.
- Prinz PU, Mendler AN, Masouris I, et al. High DGK- $\alpha$  and disabled MAPK pathways cause dysfunction of human tumor-infiltrating CD8<sup>+</sup> T cells that is reversible by pharmacologic intervention. *J Immunol* 2012;188:5990–6000.
- Ávila-Flores A, Arranz-Nicolás J, Andradá E, et al. Predominant contribution of DGK $\zeta$  over DGK $\alpha$  in the control of PKC/PDK-1-regulated functions in T cells. *Immunol Cell Biol* 2017;95:549–63.
- Andradá E, Liébana R, Merida I. Diacylglycerol Kinase  $\zeta$  Limits Cytokine-dependent Expansion of CD8<sup>+</sup> T Cells with Broad Antitumor Capacity. *EBioMedicine* 2017;19:39–48.
- Riese MJ, Wang L-CS, Moon EK, et al. Enhanced effector responses in activated CD8<sup>+</sup> T cells deficient in diacylglycerol kinases. *Cancer Res* 2013;73:3566–77.

- 30 Wesley EM, Xin G, McAllister D, *et al.* Diacylglycerol kinase  $\zeta$  (DGK $\zeta$ ) and Casitas B-lineage proto-oncogene B-deficient mice have similar functional outcomes in T cells but DGK $\zeta$ -deficient mice have increased T cell activation and tumor clearance. *Immunohorizons* 2018;2:107–18.
- 31 Arranz-Nicolás J, Mérida I. Biological regulation of diacylglycerol kinases in normal and neoplastic tissues: new opportunities for cancer immunotherapy. *Adv Biol Regul* 2020;75:100663.
- 32 Wang L-CS, Riese MJ, Moon EK, *et al.* Overcoming intrinsic inhibitory pathways to augment the antineoplastic activity of adoptively transferred T cells: Re-tuning your CAR before hitting a Rocky road. *Oncoimmunology* 2013;2:e26492.
- 33 Jutz S, Leitner J, Schmetterer K, *et al.* Assessment of costimulation and coinhibition in a triple parameter T cell reporter line: simultaneous measurement of NF- $\kappa$ B, NFAT and AP-1. *J Immunol Methods* 2016;430:10–20.
- 34 Leitner J, Kuschei W, Grabmeier-Pfistershammer K, *et al.* T cell stimulator cells, an efficient and versatile cellular system to assess the role of costimulatory ligands in the activation of human T cells. *J Immunol Methods* 2010;362:131–41.
- 35 Zhong X-P, Hainey EA, Olenchok BA, *et al.* Enhanced T cell responses due to diacylglycerol kinase zeta deficiency. *Nat Immunol* 2003;4:882–90.
- 36 Gharbi SI, Rincón E, Avila-Flores A, *et al.* Diacylglycerol kinase  $\zeta$  controls diacylglycerol metabolism at the immunological synapse. *Mol Biol Cell* 2011;22:4406–14.
- 37 Mayya V, Dustin ML. What scales the T cell response? *Trends Immunol* 2016;37:513–22.
- 38 Okamura H, Aramburu J, García-Rodríguez C, *et al.* Concerted dephosphorylation of the transcription factor NFAT1 induces a conformational switch that regulates transcriptional activity. *Mol Cell* 2000;6:539–50.
- 39 Isakov N, Altman A. Protein kinase C(theta) in T cell activation. *Annu Rev Immunol* 2002;20:761–94.
- 40 Lupino E, Ramondetti C, Piccinini M. I $\kappa$ B kinase  $\beta$  is required for activation of NF- $\kappa$ B and AP-1 in CD3/CD28-stimulated primary CD4(+) T cells. *J Immunol* 2012;188:2545–55.
- 41 Ebinu JO, Stang SL, Teixeira C, *et al.* RasGRP links T-cell receptor signaling to Ras. *Blood* 2000;95:3199–203.
- 42 Villalba M, Hernandez J, Deckert M, *et al.* Vav modulation of the Ras/MEK/ERK signaling pathway plays a role in NFAT activation and CD69 up-regulation. *Eur J Immunol* 2000;30:1587–96.
- 43 Tello-Lafoz M, Rodríguez-Rodríguez C, Kinna G, *et al.* SNX27 links DGKzeta to the control of transcriptional and metabolic programs in T lymphocytes. *Sci Rep* 2017;7:16361.
- 44 Marinari B, Costanzo A, Marzano V, *et al.* CD28 delivers a unique signal leading to the selective recruitment of RelA and p52 NF- $\kappa$ B subunits on IL-8 and Bcl-xL gene promoters. *Proc Natl Acad Sci U S A* 2004;101:6098–103.
- 45 Liao W, Lin J-X, Leonard WJ. Interleukin-2 at the crossroads of effector responses, tolerance, and immunotherapy. *Immunity* 2013;38:13–25.
- 46 Duré M, Macian F. IL-2 signaling prevents T cell anergy by inhibiting the expression of anergy-inducing genes. *Mol Immunol* 2009;46:999–1006.
- 47 Jain J, Valge-Archer VE, Sinskey AJ, *et al.* The AP-1 site at -150 bp, but not the NF- $\kappa$ B site, is likely to represent the major target of protein kinase C in the interleukin 2 promoter. *J Exp Med* 1992;175:853–62.
- 48 Carter L, Fouser LA, Jussif J, *et al.* PD-1:PD-L inhibitory pathway affects both CD4(+) and CD8(+) T cells and is overcome by IL-2. *Eur J Immunol* 2002;32:634–43.
- 49 Agata Y, Kawasaki A, Nishimura H, *et al.* Expression of the PD-1 antigen on the surface of stimulated mouse T and B lymphocytes. *Int Immunol* 1996;8:765–72.
- 50 Keir ME, Butte MJ, Freeman GJ, *et al.* PD-1 and its ligands in tolerance and immunity. *Annu Rev Immunol* 2008;26:677–704.
- 51 Freeman GJ, Long AJ, Iwai Y, *et al.* Engagement of the PD-1 immunoinhibitory receptor by a novel B7 family member leads to negative regulation of lymphocyte activation. *J Exp Med* 2000;192:1027–34.
- 52 Meng X, Liu X, Guo X, *et al.* FBXO38 mediates PD-1 ubiquitination and regulates anti-tumour immunity of T cells. *Nature* 2018;564:130–5.
- 53 Wei SC, Levine JH, Cogdill AP, *et al.* Distinct cellular mechanisms underlie anti-CTLA-4 and anti-PD-1 checkpoint blockade. *Cell* 2017;170:1120–33.
- 54 Andrada E, Almena M, de Guinoa JS, *et al.* Diacylglycerol kinase  $\zeta$  limits the polarized recruitment of diacylglycerol-enriched organelles to the immune synapse in T cells. *Sci Signal* 2016;9:ra127.
- 55 Riese MJ, Moon EK, Johnson BD, *et al.* Diacylglycerol kinases (DGKs): novel targets for improving T cell activity in cancer. *Front Cell Dev Biol* 2016;4:108.
- 56 Rincón M, Flavell RA. AP-1 transcriptional activity requires both T-cell receptor-mediated and co-stimulatory signals in primary T lymphocytes. *Embo J* 1994;13:4370–81.
- 57 Kang SM, Beverly B, Tran AC, *et al.* Transactivation by AP-1 is a molecular target of T cell clonal anergy. *Science* 1992;257:1134–8.
- 58 Shaulian E, Karin M. AP-1 as a regulator of cell life and death. *Nat Cell Biol* 2002;4:E131–6.
- 59 Mahoney KM, Freeman GJ, McDermott DF. The next Immune-Checkpoint inhibitors: PD-1/PD-L1 blockade in melanoma. *Clin Ther* 2015;37:764–82.
- 60 Spranger S, Koblisch HK, Horton B, *et al.* Mechanism of tumor rejection with doublets of CTLA-4, PD-1/PD-L1, or IDO blockade involves restored IL-2 production and proliferation of CD8(+) T cells directly within the tumor microenvironment. *J Immunother Cancer* 2014;2:3.
- 61 Jing W, Gershan JA, Holzhauer S, *et al.* T cells deficient in diacylglycerol kinase  $\zeta$  are resistant to PD-1 inhibition and help create persistent host immunity to leukemia. *Cancer Res* 2017;77:5676–86.
- 62 Parish IA, Rao S, Smyth GK, *et al.* The molecular signature of CD8+ T cells undergoing deletion tolerance. *Blood* 2009;113:4575–85.
- 63 Juneja VR, McGuire KA, Manguso RT, *et al.* PD-L1 on tumor cells is sufficient for immune evasion in immunogenic tumors and inhibits CD8 T cell cytotoxicity. *J Exp Med* 2017;214:895–904.
- 64 Tang H, Liang Y, Anders RA, *et al.* PD-L1 on host cells is essential for PD-L1 blockade-mediated tumor regression. *J Clin Invest* 2018;128:580–8.
- 65 Jung I-Y, Kim Y-Y, Yu H-S, *et al.* CRISPR/Cas9-Mediated knockout of DGK improves antitumor activities of human T cells. *Cancer Res* 2018;78:4692–703.
- 66 Martínez-Moreno M, García-Liévana J, Soutar D, *et al.* FoxO-dependent regulation of diacylglycerol kinase  $\alpha$  gene expression. *Mol Cell Biol* 2012;32:4168–80.